A Novel Adaptive Mismatch Cancellation System for Quadrature IF Radio Receivers

Li Yu, *Member, IEEE*, and W. Martin Snelgrove, *Member, IEEE*

***Abstract*— This paper investigates and resolves in-phase/quadrature phase (I/Q) imbalances between the input paths of quadrature IF receivers. These mismatches along the paths result in the image interference aliasing into the desired signal band, thus reducing the dynamic range and degrading the performance of the receivers. I/Q errors occur because of gain and phase imbalances between quadrature mixers. They are also caused by capacitor mismatches in analog-to-digital converters (A/D's), which are designed to be identical for each input path. This paper presents a novel and feasible digital signal processing (DSP) solution for the I/Q mismatch problems. The system includes a novel complex least mean square algorithm and a modified adaptive noise canceler (signal separator) to separate the desired signal and the image noise caused by the mismatch. The noise canceler can also solve the signal leakage problem, which is that the noise reference includes signal components. This system was implemented in a Xilinx FPGA and an Analog Devices DSP chip. It was tested with a complex intermediate frequency receiver, which includes an analog front end and a complex sigma–delta modulator. Both simulation results and test results show a dramatic attenuation of the image noise. Extending applications of the system to N-path systems further indicates the robustness and feasibility of this novel adaptive mismatch cancellation system.**

***Index Terms*— Image rejection, mismatch cancellation, radio architecture.**

I. Introduction

DIGITAL receivers with quadrature intermediate frequency (IF) architectures have been known for many years. This architecture has received a great deal of interest recently as a potential candidate for use in single-chip digital radio receivers [5], [24]; but it is vulnerable to mismatch. Any gain or phase imbalance between the in-phase (I) and quadrature phase (Q) paths in the system cause an image to be aliased into the passband of the signal. This problem is investigated and a novel solution is developed in this paper.

Fig. 1 shows the general structure of a modern quadrature digital wireless receiver. The desired signal is transmitted and the receiver is, unfortunately, sensitive to interference at an image frequency separated by twice the intermediate frequency from the desired signal. In general, radio designers must reject image interferers by as much as 80–100 dB [16]. One way to get this performance is to filter the image out before the mixing stage (at point A). However, for a low IF, this filter must be very selective and so becomes extremely expensive. Another method is to use in-phase/quadrature phase (I/Q) mixing or image reject mixing [17] (as shown at point B). This second technique has recently become important because high-performance filtering is harder to integrate than mixers. The problem with this structure is that it is vulnerable to gain and phase errors in the local oscillator (LO), mixer, analog-to-digital (A/D) converters, and filters, which cause image "leakage," typically degrading the performance of receivers to rejection of only about 30 dB, even with careful design. In this paper, we attempt to improve the SNR by 10–20 dB in DSP. In the example to be given, we still use the image rejection filter at point A but with easier specifications.

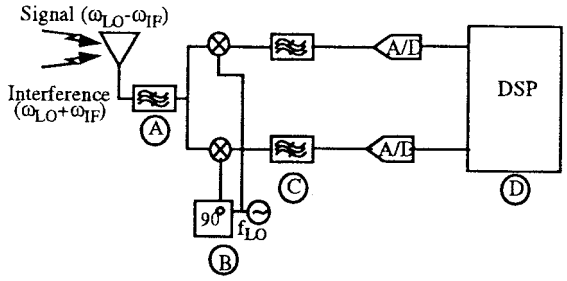

Fig. 1. Architecture of a radio receiver.

In Section II, we introduce a model of a complex IF receiver. The model includes a radio frequency (RF) front end with quadrature mixers and a two-input sigma–delta $(\Sigma\Delta)$ A/D converter as analog portions. It is difficult to achieve good balance between the I and Q paths, due to the imperfection of the analog components. Both the RF front end and the A/D converter can introduce imbalance.

Many approaches for the correction of I/Q channel imbalance have been proposed using both analog and digital methods. Modifying the analog circuitry [39], careful layout [1], and making the circuit more robust are the analog solutions introduced in [32], [14], [39]. A digital solution introduced in [9], [25] is using off-line compensation of channel imbalances. Other digital approaches, such as using the Hilbert transform to generate I/Q signals in the digital domain, are presented in [11], [27], [34].

In this paper, a novel robust adaptive mismatch cancellation system is introduced. The new system uses a new complex least mean square (LMS) algorithm and a modified adaptive noise cancellation model to compensate the signal-to-noise ratio (SNR) degradation due to the mismatch between the I and Q paths.

Both simulation and experimental results will be presented

Manuscript received May 27, 1998; revised October 13, 1998. This paper was recommended by Associate Editor P. H. Young.

L. Yu is with the Department of Electronics, Carleton University, Ottawa, ON K1S 5B6, Canada.

W. M. Snelgrove is with Philsar Electronics Inc., Ottawa, ON K1P 6K7, Canada.

Publisher Item Identifier S 1057-7130(99)04892-2.

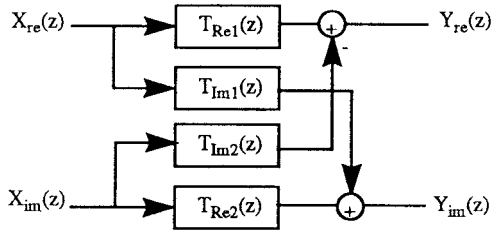

Fig. 2. Complex filter block diagram.

to confirm the feasibility of the algorithm and the system described. Finally, a real-time implementation of the system will be presented.

This paper is divided into five sections. Section I presents an introduction to I/Q channel mismatch problems. The structure of a complex IF receiver and its performance degradation due to the imbalance between the I and Q paths are introduced in Section II. I/Q mismatch problems are investigated and concepts such as complex filters, gain and phase imbalances are presented.

A novel DSP system to compensate the receiver performance degradation caused by the I/Q mismatch is developed in Section III. This section introduces the novel adaptive algorithm and the mismatch cancellation system. Previous work done on compensation of the SNR degradation for quadrature systems is reviewed. Simulation results are also included in Section III.

In Section IV, a real-time implementation of a complex IF receiver with the adaptive mismatch canceler is proposed. The novel adaptive algorithm is implemented in a DSP chip. The performance of the system is discussed with the experimental results.

Section V concludes the paper.

II. Complex IF Receivers

In this section, the basic structure of a complex IF receiver system (I/Q system) and the way mismatch affects the performance of the receiver are introduced.

A. Complex Filters

Complex filters are basic components in complex (I/Q) systems. I/Q systems can be mathematically treated as real and imaginary-valued signals. They can also be treated as filters designed with complex coefficients having nonconjugate responses. They can, however, be modeled with several cross-coupled real filters [3], [32], [14]. This is shown in Fig. 2, where the real part of the output $Y_{\rm re}(z)$ is the sum of the real part of the input $X_{\rm re}(z)$ fed through $T_{Re1}(z)$, and the imaginary part of the input $X_{\rm im}(z)$ fed through $T_{\rm Im2}(z)$; the imaginary part of the output $Y_{\rm im}(z)$ is the sum of the real part of the input $X_{\rm re}(z)$ fed through $T_{\rm Im1}(z)$, and the imaginary part of the input $X_{\rm im}(z)$ fed through $T_{Re2}(z)$. In the ideal case, $T_{Re1}(z) = T_{Re2}(z) = T_{Re}(z)$ and $T_{\rm Im1}(z) = T_{\rm Im2}(z) = T_{\rm Im}(z)$, thus the transfer function of the complex filter is $T_{\rm nom}(z) = T_{Re}(z) + jT_{\rm Im}(z)$.

Two special cases can be seen in Fig. 1.

1) The pair of real filters at point C, for which $T_{\rm im} = 0$.

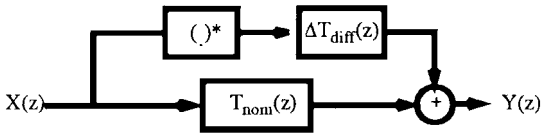

Fig. 3. Mismatch model of the complex filter.

2) The 90° phase shifter at point B. The phase shifter creates a pure positive-frequency signal $I + jQ = \cos wt + j \sin wt \equiv e^{\rm jwt}$ out of a pure-real input $coswt = \frac{1}{2}(e^{\rm jwt} + e^{-jwt})$, with power at both positive and negative frequencies. It is a "positive-pass" filter with the imaginary input "grounded." The full complex structure can be seen, e.g., in [23] and [42]. In this paper, we study the general case.

Due to imbalances or coefficient variation in the transfer functions in the system, the two real-part transfer functions are not equal in practical situations and neither are the two imaginary-part transfer functions. Therefore, the complex filter no longer simply realizes a complex transfer function. It has been shown in [3] that the transfer function of the mismatched filter can be written as a nominal term, a common-mode error term, and a differential-error term

$$Y(z) = T_{\rm nom}(z)X(z) + \Delta T_{cm}X(z) + \Delta T_{\rm diff}X(z)^* \quad (1)$$

where $X(z)^*$ is the complex conjugate of $X(z)$

$$\Delta T_{cm} = \left[\frac{T_{Re1}(z) + T_{Re2}(z)}{2} - T_{Re,\rm nom}(z)\right] + j\left[\frac{T_{\rm Im1}(z) + T_{\rm Im2}(z)}{2} - T_{\rm Im,nom}(z)\right] \quad (2)$$

and

$$\Delta T_{\rm diff} = \left[\frac{T_{Re1}(z) - T_{Re2}(z)}{2}\right] + j\left[\frac{T_{\rm Im1}(z) - T_{\rm Im2}(z)}{2}\right]. \quad (3)$$

The differential error $\Delta T_{\rm diff}$ models differential changes between $T_{Re1}(z)$ and $T_{Re2}(z)$, as well as between $T_{\rm Im1}(z)$ and $T_{\rm Im2}(z)$. It adds an error term which is a function of the complex conjugate of the input function. This is called image aliasing because it aliases signals between positive frequencies and the corresponding negative frequencies. On the other hand, the common-mode error ΔT_{cm} is used to model common changes in $T_{Re1}(z)$ and $T_{Re2}(z)$, as well as in $T_{\rm Im1}(z)$ and $T_{\rm Im2}(z)$. ΔT_{cm}can be ignored because it is usually small compared to the $T_{\rm nom}(z)$. Fig. 3 shows a mismatch model of a complex filter. $(\cdot)^*$ represents the complex conjugate operation. We will show how to cancel the image due to the $\Delta T_{\rm diff}$ path in Section III.

In the first special case of Fig. 1 (the pair of real filters), mismatched filters imply $T_{Re1} \neq T_{Re2}$ and, hence, an image is formed. Gain errors in the mixers or A/D converters have the same effect, though with a flat frequency response. For the second special case (the phase shifter), gain and phase errors in the LO paths cause the "positive pass" to leak some power at $e^{-jw_{\rm LO}t}$ through a ΔT_{cm} term. An image will still be formed.

B. Complex ΣΔ Modulators

From the previous section, we know the structure of a complex filter. Based on the complex filter theory, complex modulators can be built which have wider bandwidth than real modulators [13], [14], [31], [32]. In this paper, only complex ΣΔ modulators are discussed, again, because they give us the general case. Since a pair of conventional "real" ΣΔ modulators just have $T_{\rm im}$ terms zero, and Nyquist converters are simpler with no noise transfer function (NTF) to consider, in this paper, only complex ΣΔ modulators are discussed to cover the general case. ΣΔ modulation is a modulation scheme based on ΣΔ A/D conversion technology which has oversampling and noise shaping characteristics [7].

1) Advantages of Complex Bandpass ΣΔ Modulators: A complex bandpass ΣΔ modulator is a bandpass ΣΔ modulator which has a complex NTF. A complex NTF can achieve better performance than a real NTF for a given order or numbers of zeros [4], because the bandwidth of the modulator depends on the number of the zeros in the band of interest, and because a complex NTF is not constrained to realize the zeros in complex conjugate pairs, all its zeros can be put in the band of interest. For example, a fourth-order complex filter has almost the same bandwidth as an eighth-order real NTF in the real frequency band but is more stable [31]. In terms of complexity, using the fourth-order real NTF would involve two modulators (for I and Q) for a total of eight integrators, the same complexity as the fourth-order complex case.

2) Mismatch in Complex ΣΔ Modulators: In the presence of mismatch in the signal or NTF's in a complex ΣΔ modulator, signals or noise at the image frequency will alias into the band of interest. For complex bandpass ΣΔ modulators, this situation is more serious because their frequency responses are asymmetric and the notches at the image band are usually much shallower than their real parts. Fig. 4 shows the output spectrum of a complex bandpass ΣΔ modulator ($fs = 80$ MHz), with and without a 1% coefficient mismatch in the NTF [31]. Coefficient mismatch refers to the coefficient differences between $T_{Re1}(z)$ and $T_{Re2}(z)$, as well as $T_{\rm Im1}(z)$ and $T_{\rm Im2}(z)$. In switched-capacitor circuits, these coefficients are implemented with capacitors. Thus, coefficient mismatch is caused by the imperfection of the capacitors. It can be seen that with a 1% coefficient mismatch, the SNR is degraded by 35 dB.

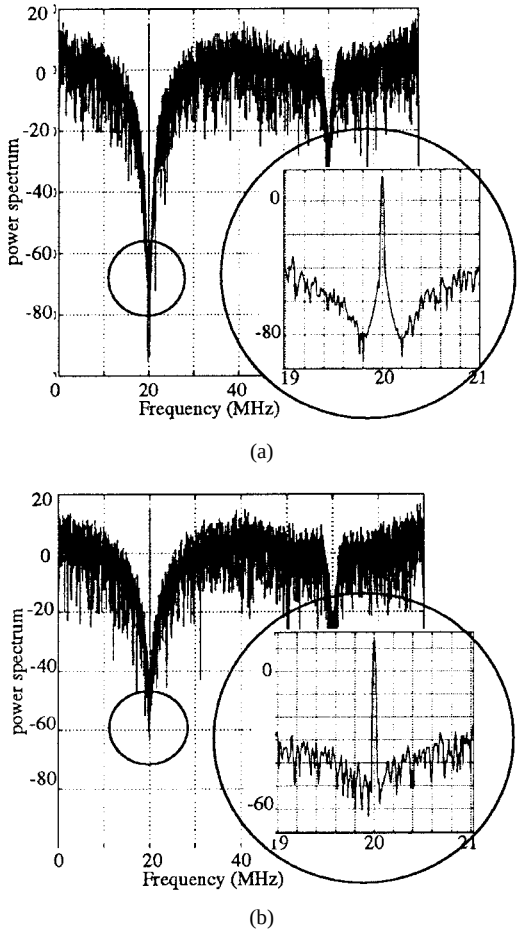

Fig. 4. Output spectra of a fourth-order ΣΔ modulator. (a) Ideal case (SNR=100 dB). (b) With 1% coefficient mismatch (SNR=65 dB).

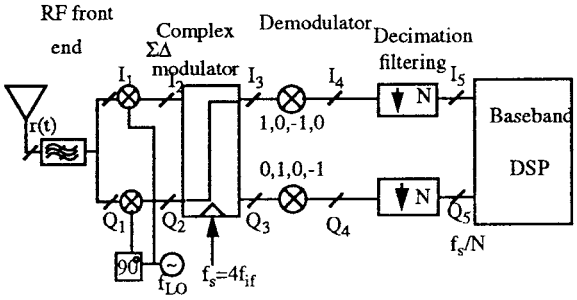

Fig. 5. Single IF receiver structure.

C. Complex IF Receiver

1) Structure of a Single IF Receiver: Based on the complex ΣΔ modulator introduced in the previous section, we can build a single IF receiver. The structure of the receiver is shown in Fig. 5 [30], [33], [36]. We use the digital complex sampling technique [23], also called digital quadrature demodulation, in the demodulation process of this quadrature IF receiver. Digital complex sampling is a technique which uses IF sampling to produce baseband I and Q signals. The IF signal is sampled at approximately four times the IF center frequency, and the samples are sorted into I and Q data streams. The quadrature sinusoidal used to demodulate the IF signal simply become sequences of $(1, 0, -1, 0, \cdots)$ and $(0, 1, 0, -1, \cdots)$, respectively. This can be easily implemented without using multipliers, resulting in minimal hardware [22].

I_1 and Q_1, which are the same at the downconverter inputs, are RF signals which are at 1.9 GHz according to the Personal Communications Services (PCS) standard. I_2 and Q_2 are IF signals which are generated through mixing I_1 and Q_1 with $f_{\rm LO}$. I_3 and Q_3 are quantized versions of I_2 and Q_2 represented as 1-bit streams. Using digital quadrature demodulation, I_4 and Q_4 are baseband signals but still 1-bit streams at a high sampling rate. After decimation filtering, I_5 and Q_5 are n-bit streams at a Nyquist sampling rate.

2) Mismatch Problems: The outputs I_3 and Q_3 of the two paths should have the same amplitude and 90° phase differ-

TABLE I
RECEIVER PARAMETERS. BANDWIDTH–TIME PRODUCT. B IS THE 3-dB BANDWIDTH OF THE GAUSSIAN FILTER AND T IS THE SYMBOL PERIOD. BT=0.3 IS SPECIFIED IN THE GSM STANDARD

Parameter	Value
RF Frequency	1.9GHz
LO f_{lo}	1.91GHz
Sampling Frequency f_s	40MHz
Modulation Scheme	GMSK
Data rate	270.833 kb/s
BT[a]	0.3
Decimation rate	64

ence. But mismatches can occur at many locations in the receiver, shown in Fig. 5. For example, take the RF front end, the main component is the mixer. It uses two sinusoids at the LO frequency that are nominally equal in amplitude, with a 90∘ phase difference. In practice, these two sinusoids are always unbalanced because high-precision phase matching is difficult to achieve in analog circuitry. The effect of this imbalance is to generate an image, which can limit the dynamic range of a receiver [35].

In addition to gain or phase imbalances in the mixer, capacitor mismatch is also a big concern in the analog system. Coefficients in the transfer functions are realized by capacitors in switched-capacitor circuits, so capacitor mismatch will result in coefficient mismatch. As shown in Fig. 3, with the coefficient mismatch in the transfer functions of the complex $(\Sigma\Delta)$, the image noise will be aliased into the signal band through the upper path in the model.

3) Interference: During the mixing stage, the desired signal at f_{RF} is mixed with local oscillator signal at f_{LO} to produce an IF signal at $f_{\mathrm{IF}} = f_{\mathrm{LO}} - f_{\mathrm{RF}}$. However, some signals at a certain frequency f_{image}, such as $f_{\mathrm{RB}} + 2f_{\mathrm{IF}}$, can be mixed with f_{LO} to produce an image interference at $-f_{\mathrm{IF}}$. When there is no mismatch between the two paths, this image interference has no effect on the performance of the system. But if there is a gain, phase, or coefficient imbalance in any part of the system, this image interference will alias into the desired signal band. This will limit the selectivity of the receiver.

4) Examples: To study the mismatch phenomenon in a single IF receiver, this paper proposes a technique and analyzes, simulates and builds a prototype. The test example is based on DCS-1800 (GSM-like) in the receiver proposed by Swaminathan [31], [42]. The architecture of the receiver shown in Fig. 5. Table I shows the parameters used in the receiver. The signal bandwidth after decimation filtering is about 312.5 kHz, which can be used in a GSM receiver [21]. The data rate in the GSM standard is 270.833 kb/s.

The desired signal and interference signal for our example are, respectively, shown in Table II. Fig. 6 is the spectrum of the output of the $(\Sigma\Delta)$ modulator $I_3 + jQ_3$, with the desired signal and its image interference, when there is no mismatch

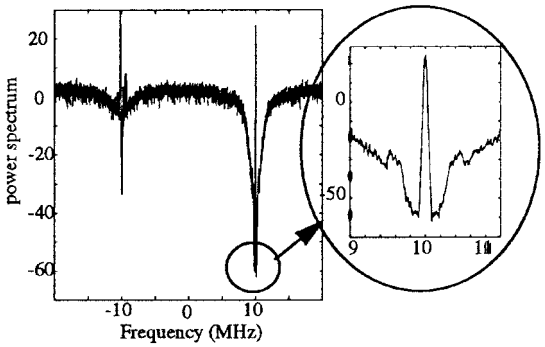

Fig. 6. Output spectra of the complex $\Sigma\Delta$ modulator.

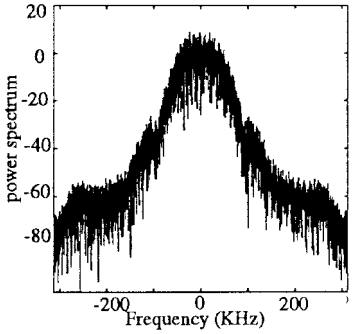

Fig. 7. Magnitude response of $I_5 + jQ_5$.

between I and Q paths. An expanded frequency response in the band of interest (9–11 MHz) is shown next to it. The desired signal tone is at 10 MHz after being mixed from the RF down to the IF band. The interference signal is at -10 MHz.

Fig. 7 is the spectrum of the received signal after decimation. This demonstrates that when the I and Q paths are perfectly balanced, the image interferer has no effect on system performance.

Fig. 8(a) is the eye diagram of the transmitted baseband signal, and Fig. 8(b) is the eye diagram of the received signal. It can be seen that the received signal is a delayed version of the input signal. For this ideal case, the interference has no effect.

Figs. 9 and 10 show the effects of mismatch. Comparing Figs. 9(a) and Fig. 6(a), it can be seen that with mismatches between the I and Q paths, not only is the noise floor increased, but also the frequency modulation (FM) interference is aliased into the region 10.15–10.25 MHz. The recovered baseband signal is shown in Fig. 9(b), which shows the image aliasing located in the band 150–250 kHz. The SNR is about 30 dB, which represents a degradation of more than 30 dB compared to the ideal case. The spectra shown in Fig. 9 are obtained with the interference offset by 200 kHz, so that the reader can distinguish it from the GMSK signal. In this case, of course, conventional filtering could remove it and the problem would not be serious. We will show more results with no offset in the interference in Section III. Fig. 10 shows the eye diagrams of the corrupted signal. It can be seen that the eyes are modulated by the image interference. The performance degradation is obvious. In the next section, we

TABLE II
DESIRED SIGNAL AND INTERFERENCE

desired signal		interference	
modulation scheme	GMSK	modulation scheme	FM
bit rate	270.833 kb/s	bandwidth	100kHz
carrier frequency	1.9GHz	carrier frequency	1.9202GHz

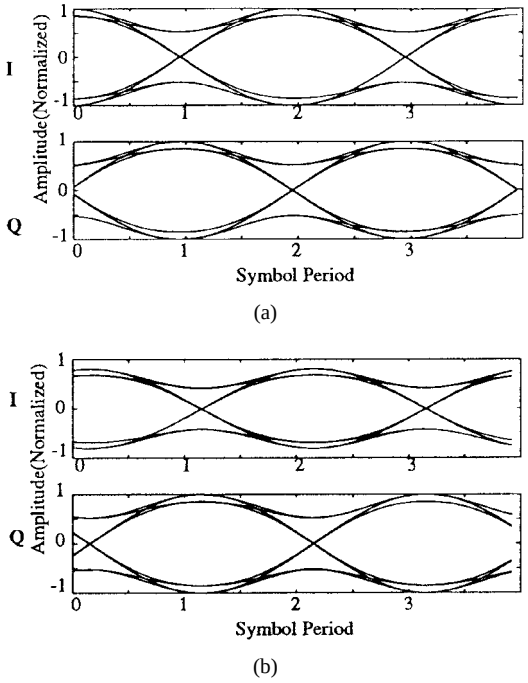

Fig. 8. Comparison of the eye diagrams between the input signal and the received signal: no mismatch, but with interferer, the eye diagram is unaffected by the interferer. (a) Eye diagram of the input symbol. (b) Eye diagram of the received signal.

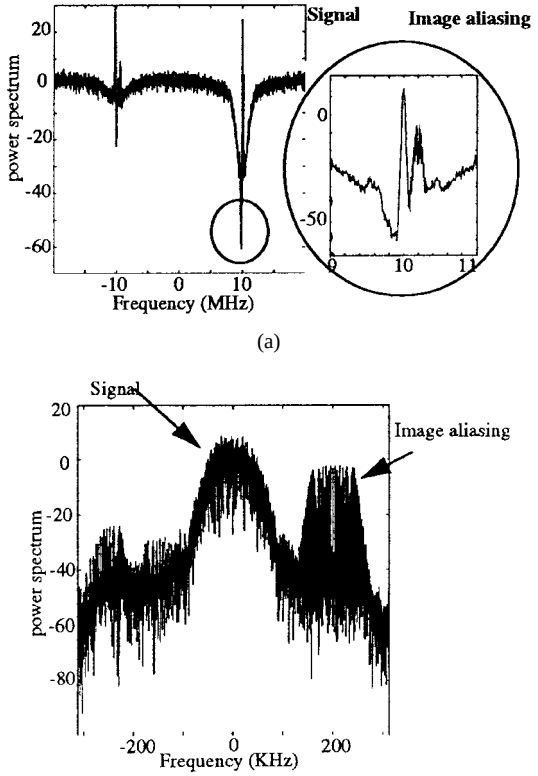

Fig. 9. Output spectra with mismatch. (a) Output of the complex modulator. (b) Output signal after decimation.

will introduce a DSP solution to cancel the mismatch and enhance the performance.

III. AN ADAPTIVE ALGORITHM FOR I/Q CHANNEL MISMATCH CANCELLATION

In the previous section, we analyzed the mismatch problems in the complex system. In this section, we are going to present a novel DSP solution for this problem. Using a modified adaptive noise cancellation model and a new adaptive algorithm, the degradation due to the I/Q channel mismatch can be effectively compensated.

A. Previous Solutions

In quadrature sampling systems, the I/Q channel mismatch problem is always a big concern. A large amount of work has been done to minimize the degradation due to the channel mismatch.

1) Off-Line Adjustment: If the imbalance of the two paths can be measured, it can be corrected. The correction scheme is through the Gram–Schmidt procedure, which produces an orthonormal basis from an arbitrary set of vectors [34], [8], [26]. In [10], Churchill presented a method that uses the Gram–Schmidt procedure to correct I/Q problems. This correction can be applied one frequency at a time. When the I and Q channels cover a wide bandwidth, the imbalance is a function of frequency. This method might be impractical to apply because it needs an off-line test input and can not track time variation.

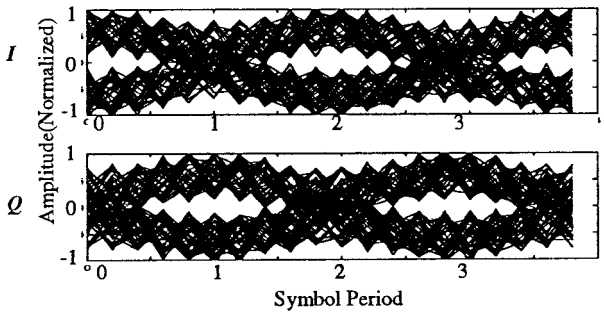

Fig. 10. Eye diagrams of the degraded I, Q signal.

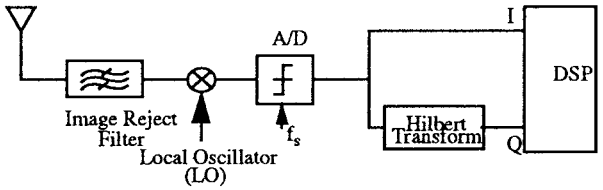

Fig. 11. A digital receiver with Hilbert transform.

2) Hilbert Transform: A solution mentioned in [35] is to move the generation of I and Q signals to the digital domain by using the Hilbert transform [8], [15], [18], [19], [22]. The structure of this kind of receiver is shown in Fig. 11. In this approach, the data for one channel (say the I channel) are obtained from a single-path A/D converter, while the data of the Q channel are generated by processing the I channel data through a Hilbert filter. Since the Q channel data are generated digitally, the imbalance between the outputs of the I and Q channels can be kept at a minimum.

One of the major disadvantages of this approach is that the operating speed is limited by the complexity of Hilbert filters. In order to get balanced I and Q signals, a high-order filter is needed to perform the Hilbert transform. The resulting solution has high power consumption, low processing speed, and high hardware complexity. More importantly, the system now has a single-path mixer and therefore relies entirely on a filter to control the image at $f_{\rm RF} \pm 2f_{\rm IF}$.

3) An Improved $\Sigma\Delta$ Modulator Structure: Another technique is to compensate for part of the performance degradation due to mismatch in complex sigma–delta modulators. One of the NTF notches is placed in the quantizer's own image band, which provides some attenuation of the image band noise before it aliases into the desired signal band [14]. However, this kind of improvement does not have much effect on the interference that exists at the image frequency because it involves only the transfer functions for quantization noise. This is explained as follows. The output of the complex sigma–delta modulator Y can be simply expressed as

$$Y = GX + HE \tag{4}$$

where X is the input of the complex sigma–delta modulator, E is the quantization noise, G is the signal transfer function (STF) and H is the NTF.

When there is a mismatch, (4) can be written as

$$Y = GX + \Delta G_{\rm diff} X^* + HE + \Delta H_{\rm diff} E^* \tag{5}$$

where $(\cdot)^*$ is the complex conjugate, and $\Delta G_{\rm diff}$ and $\Delta H_{\rm diff}$ are the differential error term of transfer functions G and H, respectively.

By placing one of the four notches in the image band, only H has been improved such that E^* gets attenuated by $\Delta H_{\rm diff}$ before it aliases into the signal band. The other differential error term $\Delta G_{\rm diff} X^*$ has not been considered. If there is a strong interference at the image frequency, image aliasing due to this term cannot be ignored.

Next, we introduce a new method to improve the SNR in the unbalanced I/Q system. The method uses the fact that the analog circuitry error can be compensated in the digital world. It takes advantage of the complex system and uses the adaptive noise cancellation model to get best performances.

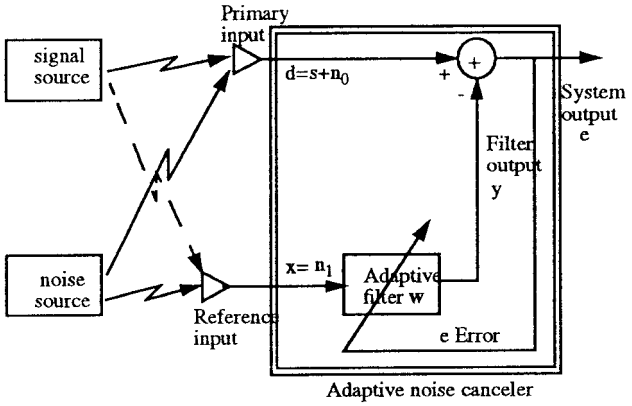

Fig. 12. Adaptive noise cancellation model.

B. An Adaptive Noise Canceler System

We propose to use adaptive filtering to correct mismatches. A simple case is an adaptive noise canceller, shown in Fig. 12. A signal is transmitted over a channel to a sensor that receives the signal s plus an uncorrelated noise n_0. The combined signal and noise $s+n_0$ form the primary input of the canceler.

A second sensor receives a noise n_1 which is uncorrelated with the signal s, but is correlated in some unknown way with the noise n_0. This sensor provides the *reference input* to the canceler. The noise n_1 is filtered to produce an output y that is a close replica of n_0. This output is subtracted from the *primary input* $s + n_0$ to produce the system output e, which is equal to $s + n_0 - y$.

If one knew the characteristics of the channels over which the noise was transmitted to the primary and reference sensors, one could, in general, design a fixed filter capable of changing n_1 into $y = n_0$. The filter output could then be subtracted from the *primary input*, and the system output would be the signal alone.

In the system shown in Fig. 12, the *reference input* is processed by an adaptive filter that automatically adjusts its own impulse response through an adaptive algorithm [37] such as LMS to the transfer function between n_1 and n_0. Thus, with the proper algorithm, the filter can operate under changing conditions and readjust itself continuously to minimize the error signal.

C. A Modified Adaptive Noise Canceler Model

How do we fit this model to our complex system to minimize the image noise due to channel mismatches?

In our system shown in Fig. 3, the noise or interference we are trying to eliminate comes from the differential error term. The perfect *reference input* signal would be the complex conjugate of the input signal $X(z)$. We have to notice that the input signal for the complex modulator is an analog signal and it will not be available as the *reference input* in the DSP system. The only way we can get the digitized complex conjugate of the input signal is from the output signal of the modulator. To simplify the equation, we use a

complex representation, therefore, all the variables and transfer functions in the following expressions are complex. The output of the modulator $Y(z)$ can be expressed as

$$Y = GX + \Delta G_{\text{diff}} X^* + HE + \Delta H_{\text{diff}} E^*. \tag{6}$$

where X is the input of the complex sigma–delta modulator, E is the quantization noise, G is the STF and H is the NTF. ΔG_{diff} and ΔH_{diff} are the differential error term of transfer functions G and H, respectively, so that

$$Y^* = G^* X(z)^* + \Delta G^*_{\text{diff}} X(z) + H^* E(z)^* + \Delta H^*_{\text{diff}} E(z). \tag{7}$$

1) Problems in the Classic Model: If we choose $Y(z)^*$ as the *reference input*, it can be seen from (7) that $Y(z)^*$ not only has the component of the complex conjugates of the desired signal, $X(z)^*$, but also the desired signal itself, $X(z)$, which means directly applying the algorithm will not only suppress the image noise but also attenuate the signal itself. The SNR improvement is impaired because this biases the filter coefficients. This phenomenon in adaptive signal processing is called signal leakage and it is represented by the dotted line in Fig. 12 [37].

According to Widrow *et al.* [37], assuming the noises in *primary* and *reference inputs* are mutually correlated, the SNR at the noise-canceler output, which is e in Fig. 12, is simply the reciprocal at all frequencies of the SNR at the *reference input*, which is x

$$\rho_{\text{out}}(z) = \frac{1}{\rho_{\text{ref}}(z)} \quad [37] \tag{8}$$

where $\rho_{\text{out}}(z)$ is the signal-to-noise ratio at the output and $\rho_{\text{ref}}(z)$ is the signal-to-noise ratio at the *reference input*. This process in (8) is called *power inversion* [37].

Smaller signal leakage means there is less signal component at the *reference input*. The SNR density ratio ρ_{ref} is smaller. The output SNR will be larger.

For our system, the *primary input* is the output of the complex filter with the image aliasing, $Y(z)$. The signal is $X(z)$ and the image noise is $\overline{X(z)}$. Thus, the SNR at the *primary input* is

$$\rho_{\text{primary}}(z) = \left| \frac{G(z)}{\Delta G_{\text{diff}}(z)} \right|$$

where $\rho_{\text{primary}}(z)$ is the signal-to-noise ratio at the *primary input*. While the complex conjugate of the output is assigned as the *reference input*, the SNR at the *reference input* is

$$\rho_{\text{ref}}(z) = \left| \frac{\Delta G_{\text{diff}}(z)^*}{G(z)^*} \right| = \left| \frac{\Delta G_{\text{diff}}(z)}{G(z)} \right|.$$

According to (8), the SNR at the adaptive noise canceler output is

$$\rho_{\text{out}}(z) = \frac{1}{\rho_{\text{ref}}(z)} = \left| \frac{G(z)}{\Delta G_{\text{diff}}(z)} \right| = \rho_{\text{primary}}(z).$$

If the classic adaptive noise cancellation system is connected after the complex filter, the output of the system has the same SNR as the output of the complex filter, which means the power of the image noise over the power of the desired signal is unchanged. There is then no point in adding the adaptive noise cancellation system.

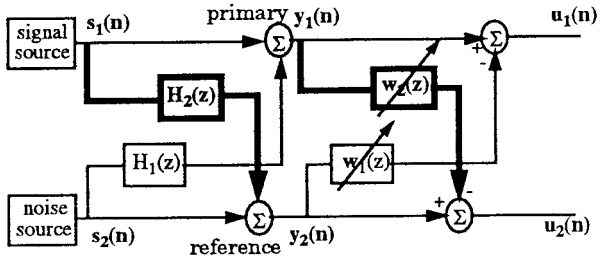

Fig. 13. Modified adaptive noise cancellation model.

2) Improved Model: The derivation above shows that we need to modify the classic noise canceler to a signal separator, which can separate the desired signal and the noise reference and get a "clean" signal and reference. "Clean" means they are uncorrelated to each other.

The classic noise canceler model in Fig. 12 is based on the correlation between the *reference input* n_1 and n_0 of the *primary input*. The adaptive filter models this correlation function. Now the reference input has some signal components that are correlated with the desired signal s. The modified model also considers this correlation and adds another adaptive filter modeling this correlation function. The modified system is called a signal separation system. The signal separation system is shown in Fig. 13 [11]. Here, we assume that two signals $y_1(n), y_2(n)$ can be written as

$$y_i(k) = s_i(k) + \boldsymbol{h}_i(k) \otimes s_j(k), \qquad i = 1,2, \quad j = 2,1 \tag{9}$$

where $s_1(k)$ and $s_2(k)$ are uncorrelated. Both $y_1(k)$ and $y_2(k)$ have $s_1(k)$ and $s_2(k)$ components. "$\otimes$" represents convolution. The signal leakage problem can be modeled by (9).

The aim for the modified noise cancellation system is to obtain signal estimates $u_i(k)$ by adaptive filtering of $y_i(k)$. The bold parts in Fig. 13 show differences between the improved model and the traditional noise canceler. The signal estimates $u_i(k)$ can be written as

$$u_i(k) = y_i(k) = \boldsymbol{w}_i^T(k) \otimes y_j(k), \qquad i = 1,2 \quad j = 2,1 \tag{10}$$

where $\boldsymbol{w}_i(k)$ is the coefficients of the adaptive filters, expressed as

$$\boldsymbol{w}_i(k) = [w^{(k)})i(0)w^{(k)})i(1) \cdots w_i^{(k)}(L_i - 1)]^T$$

and L_i is the order of the adaptive filter

$$\boldsymbol{y}_i(k) = [y_i(k) y_i(k-1) \cdots y_i(k - L_i + 1)]^T.$$

The coefficients' updates are

$$\begin{aligned} w_1^{(k+1)}(m) &= w_1^{(k)}(m) + \mu_1(k) u_2(k-m), \\ &\qquad m = 0 \cdots (L_1 - 1) \\ w_2^{(k+1)}(n) &= w_2^{(k)}(n) + \mu_2 u_2(k) u_1(k-n), \\ &\qquad n = 0 \cdots (L_2 - 1). \end{aligned} \tag{11}$$

Equation (11) uses "u_2," where a simple noise canceller would use "y_2." The signal leakage term has been cancelled in "u_2" so that updates for $\boldsymbol{w}_1$ are not biased by it.

D. Complex LMS Algorithm

The adaptive algorithm chosen here is the LMS algorithm, because of its simplicity, hardware efficiency and stability [37]. More sophisticated algorithms converge and track more rapidly, but typical mismatch mechanisms depending on device ratios and temperature differences do not need to be tracked very rapidly. Because the systems we are dealing with here are complex systems, the complex LMS algorithm will be introduced next.

Based on the modified model proposed in Section III-C.2, the modified complex LMS algorithm can be expressed as follows. All expressions of the variables or adaptive filters follow the notations in Fig. 13.

The system outputs $u_i(k) = u_{iR}(k) + ju_{iI}(k)$, can be expressed as

$$u_i(k) = y_i(k) - \boldsymbol{y}_j^T(k) \otimes \boldsymbol{w}_i(k), \quad i = 1,2, \quad j = 2,1. \tag{12}$$

The *primary input* vector $\boldsymbol{y}_1(k)$ and the *reference input* vector $\boldsymbol{y}_2(k)$ are written as

$$\boldsymbol{y}_i(k) = \boldsymbol{y}_{iR}(k) + j \cdot \boldsymbol{y}_{iI}(k), \quad i = 1,2.$$

The coefficient update equation can be written as

$$\boldsymbol{w}_i(k+1) = \boldsymbol{w}_i(k) + 2\boldsymbol{\mu}_i u_i(k) \boldsymbol{u}_j(k)^*, \quad i = 1,2, \quad j = 2,1. \tag{13}$$

$\boldsymbol{\mu}_i$ are the stepsizes which control the speed and stability of adaptation of the real part and imaginary part of the coefficients respectively. The system outputs, the "clean" signal and noise vectors are $\boldsymbol{u}_i(k) = \boldsymbol{u}_{iR}(k) + j\boldsymbol{u}_{il}(k)$. The coefficients of the adaptive filters are

$$\boldsymbol{w}_i(k) = \boldsymbol{w}_{iR}(k) + j \cdot \boldsymbol{w}_{il}(k)$$

where

$$\boldsymbol{w}_{iR}(k) = [w_{iR}^{(k)}(0) w_{iR}^{(k)}(1) \cdots w_{iR}^{(k)}(L_i - 1)]^T$$
$$\boldsymbol{w}_{iI}(k = [w_{iI}^{(k)}(0) w_{iI}^{(k)}(1) \cdots w_{iI}^{(k)}(L_i - 1)]^T.$$

L_i is the order of the adaptive filter.

1) Decimation Filtering: $\Sigma\Delta$ modulators have noise-shaping characteristics, i.e., the quantization noise can be shaped out of the band of interest. We can see from Fig. 4(b) that the out-of-band quantization noise is much larger than the image noise due to mismatches. If we directly apply the outputs from the $\Sigma\Delta$ modulator to the noise cancellation system, the *primary input* contains a large amount of quantization noise, which is uncorrelated with the interference signal, and the out-of-band quantization noise floor can be higher than the interference level. This will make the coefficients in the adaptive filter converge to zeros instead of converging to the coefficients that can eliminate the mismatch. One way to solve this problem is to use bandpass filters to obtain only the information in the band of interest. The system architecture is shown in Fig. 14. The bandpass filters are added before the mismatch cancellation system. Fig. 15 shows the simulation result of applying the new algorithm to the previous example in Fig. 4 with 1% coefficient mismatch. We can see

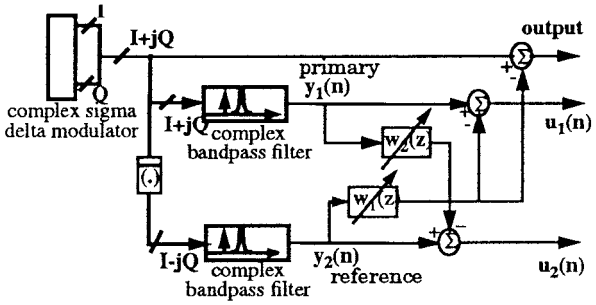

Fig. 14. Block diagram of the mismatch cancellation system (using bandpass filters).

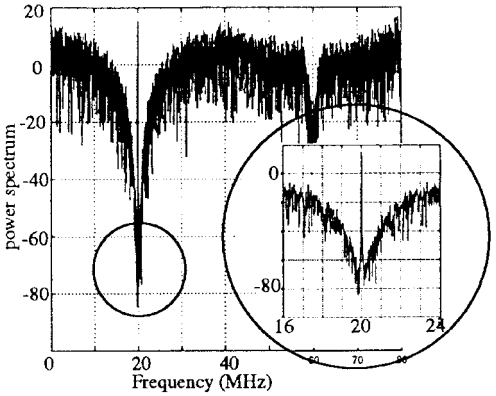

Fig. 15. Output spectrum after the mismatch cancellation.

the noise floor is brought down to -70 dB. Hence, a 20-dB improvement has been achieved. Bandpass filters used in the simulation eliminate the quantization noise and leave the desired signal and image noise due to the mismatch untouched. But these bandpass filters are very difficult and expensive to implement in real time, because they work at very high speed (40 MHz in the example).

Recall the receiver structure shown in Fig. 5 of Section II, in which the demodulator and decimation filters are used for getting rid of quantization noise and bringing the IF signal to the baseband. Thus, we can remove the bandpass filters and take advantage of demodulator and decimation filters.

If we can move the noise cancellation system after the decimation filters, the operating frequency can go down to 625 kHz in the example, and the complex bandpass filters shown in Fig. 14 are no longer necessary. This means the system is operating at same rate as the decision feedback equalizer (DFE), which is in the system anyway. Thus, the novel correction system is a reasonable load for the receiver.

Decimation filtering for $\Sigma\Delta$ modulators has been studied in [7], [24]. The simplest and most economical filter to reduce the input sampling rate is a cascaded integrator-comb (CIC) filter proposed by Hogenauer [12], because such a filter does not require a multiplier. A CIC decimation filter consists of two main sections: an integrator section, which is a cascade of L integrators with the transfer function

$$H_I(z) = \left(\frac{1}{1 - z^{-1}}\right)^L$$

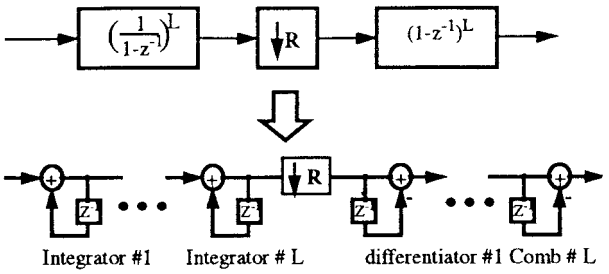

Fig. 16. Block diagram of a CIC decimation filter.

and a comb section, which is a cascade of L combs with the transfer function

$$H_c(z) = (1 - z^{-1})^L.$$

The integrator and comb sections are separated by a decimator with a decimation factor R. The structure of this filter is shown in Fig. 16. It is very suitable for very large-scale integration (VLSI) implementation at high data rates because of the simplicity of this filter and its efficient structure. Additionally, the comb section operates at the lower data rate, resulting in a smaller chip area and lower power dissipation.

Thus, the modified algorithm not only can improve the system performance by compensating the degradation due to mismatch, but can do so in a very efficient way.

E. A Simulink Model for the Complex A/D and the Modified Algorithm

Fig. 17 shows the MATLAB model and the spectrum at each stage. The desired signal generated from a GMSK random source is modulated to an RF frequency f_{RF}. The image interference generated from an FM source is modulated to $f_{\mathrm{RF}} + 2f_{\mathrm{IF}}$. After passing through the mixer shown in part II of Fig. 17, the signal and the image interference are located at f_{IF} and $-f_{\mathrm{IF}}$, respectively, which can be clearly seen from the spectra.

The output of the complex bandpass sigma–delta modulator is an oversampled 1-bit data stream, which has a deep notch at f_{IF} and an asymmetric frequency response at $-f_{\mathrm{IF}}$ shown in Section III of Fig. 17. The image aliasing due to the mismatch can also be seen at this stage.

Section IV is a digital quadrature demodulator, of which the output is a baseband signal sampled at the oversampling rate. After the decimation, the sampling rate is back to the Nyquist rate. The magnitude responses of the outputs after the decimation, including the *primary input* and the *reference input* for the adaptive mismatch cancellation system, are shown in Section V.

The corrected signal is shown in Section VI.

F. Simulation Results

This section will present results using the MATLAB model shown in Fig. 17 to prove the feasibility of the novel adaptive mismatch cancellation system. The adaptive mismatch cancellation system operates on the signal, $I_5 + jQ_5$. After applying the system, the improvements of $I_5 + jQ_5$ are presented in this section. The magnitude response of $I_5 + jQ_5$ in the absence of

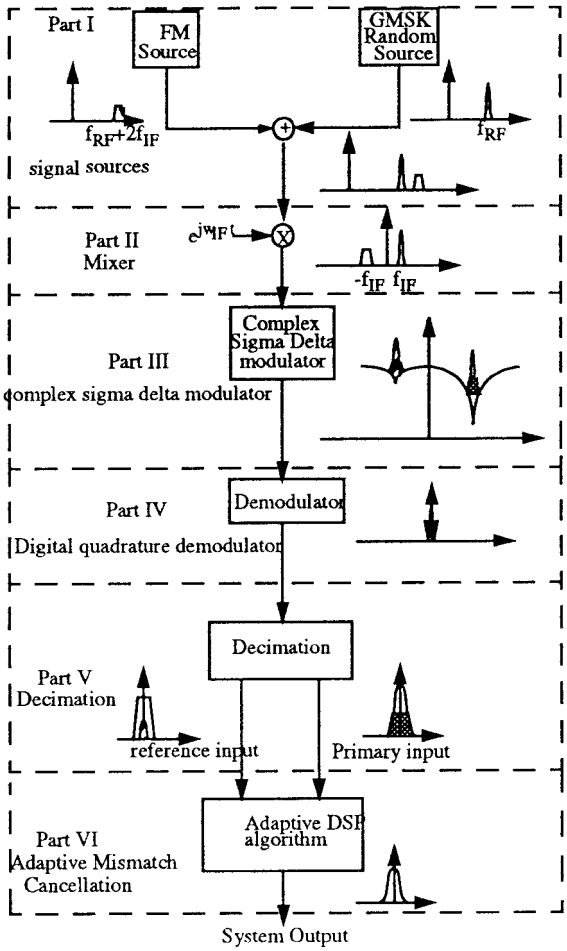

Fig. 17. Matlab module and signal spectrum in each stage.

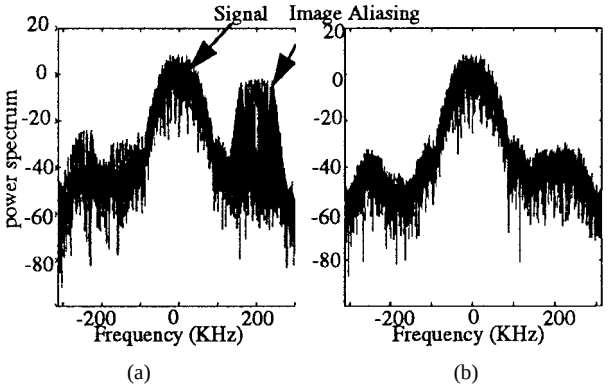

Fig. 18. Output spectra before and after using the mismatch cancellation system. (a) With mismatch. (b) After mismatch cancellation.

the mismatch cancellation system is shown in Fig. 18(a). The image aliasing can be clearly seen. This is an artificial example with the FM interference moved 200 kHz off the image frequency so that the signal and interference can be visually separated. In this case, of course, conventional filtering would suffice. The SNR in this case is about 30 dB. Fig. 18(b) shows the output spectrum after the mismatch cancellation. It can be seen that the image aliasing gets significant attenuation after applying the mismatch cancellation system. The SNR is increased to 52 dB, which implies an SNR improvement

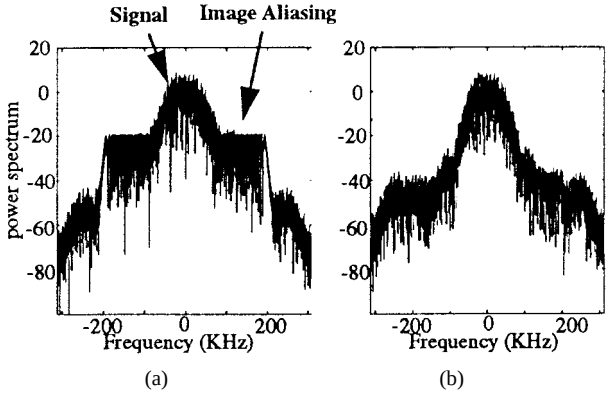

Fig. 19. Output magnitude responses before and after the mismatch cancellation system. (a) With mismatch. (b) After the mismatch cancellation system.

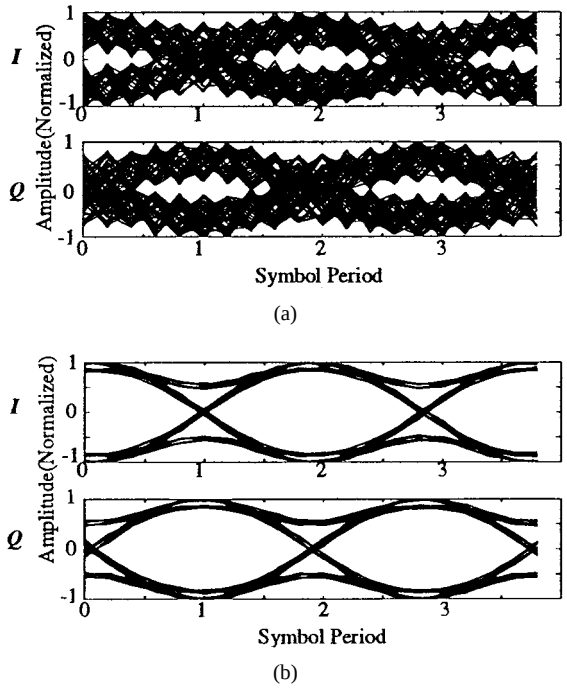

Fig. 20. Eye diagrams before and after mismatch cancellation. (a) Eye diagrams with mismatch. (b) Eye diagrams before and after mismatch cancellation.

of more than 20 dB. Fig. 19(a) shows a more realistic scenario, with overlapped signal and image. Fig. 19(b) shows the improved output after applying the proposed mismatch cancellation system.[1]

Dramatic improvement can also be seen from comparison of the eye diagrams of the outputs in Fig. 18(a) and (b).

Fig. 20(a) shows the eye diagrams of the I and Q outputs before applying the new mismatch cancellation system. We can see in the eye diagrams that the image interference (FM signal) has corrupted the desired GMSK signal. The eyes are only half-open and ambiguous. In Fig. 20(b) it can be seen that after using the presented adaptive system, the eyes are wide open and clear, which means most of the image interference has been removed.

[1]This figure shows an FFT of the last 10K samples of a 200K-point simulation.

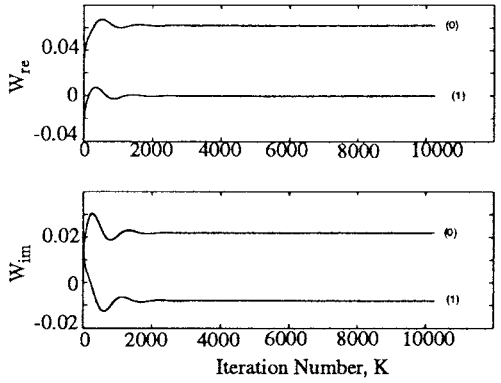

Fig. 21. Coefficients of the adaptive filter.

The convergence curves of coefficients of the adaptive filter are shown in Fig. 21. Only the coefficients of $\boldsymbol{w}_1(z)$ are presented because of the symmetric structure of the modified adaptive system in Fig. 13. In this example, the adaptive filter is a first order (two-tap) complex adaptive FIR filter. The upper part in Fig. 21 shows the real part of the coefficients, while the lower part shows the imaginary part of the coefficients.

From the simulation results shown in this section, it is clear that the novel system works efficiently and powerfully.

IV. A Real-Time Implementation

This section describes a real-time implementation of the novel DSP mismatch cancellation system proposed in Section III. The target application is a complex IF receiver. This implementation proves that the technique works well in the presence of all of the impairments of a practical system, such as circuit noise, offsets, drifts, and distortions.

A. The Test System Architecture

The test example is based on DCS-1800 (GSM) in the receiver proposed by Swaminathan [31], [41]. The overall performance of this testing prototype is limited by the available components and restricted choice of IF. This paper focuses on DSP correction of mismatch.

The block diagram of the testing hardware is shown in Fig. 22. The details of each part will be presented in the following.

The analog front end consists of a monolithic LNA [16], notch filter [17], and quadrature mixer [31] implemented in a 0.8-μm BiCMOS process with on-chip inductors.

The complex $\Sigma\Delta$ modulator used in the implementation is a fourth order modulator which has three zeros in the real band and one zero in the imaginary band in order to attenuate the image noise before it aliases into the real band [31].

The $\Sigma\Delta$ modulator is an oversampled one-bit A/D converter. A decimation filter which uses the proposed structure for the decimation filters introduced in Section III-D1 is needed to convert the one-bit stream at the oversampling rate to an n-bit word at the Nyquist rate.

The implementation of the novel adaptive mismatch cancellation algorithm uses an evaluation kit [2] provided by Analog Devices, which has an Analog Devices ADSP-21 020 32-bit

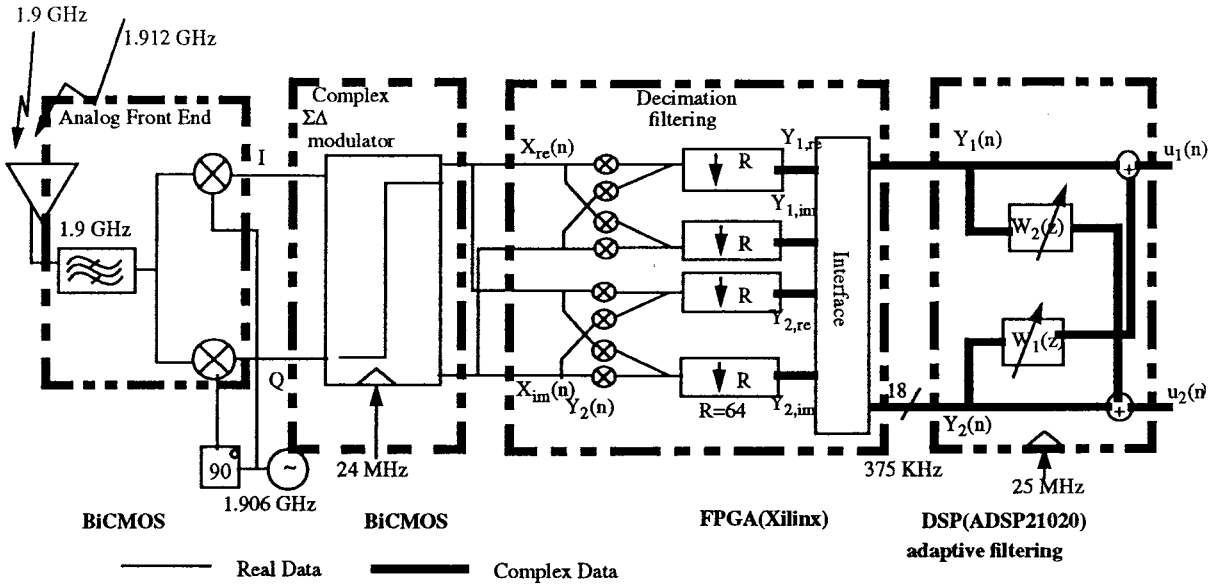

Fig. 22. Hardware system for testing.

floating point signal processor operating at 33 MHz, an in-circuit emulator, and a PC. The algorithm is coded in the DSP's assembly language.

The algorithm proposed in Section III-C2 can be implemented with ASIC technology. If two-tap complex adaptive filters are chosen, there are four multiplications and four additions for each complex adaptive filter. Thus, there are eight multiplications and eight additions for each Nyquist sample. It can be seen that the reference path can be very simple because u_1 is the desired output and the u_2 is the image noise. Thus, the complex filter $\boldsymbol{w}_2$ can be of zeroth order and the multiplier does not need to be very accurate. Receivers usually have enough DSP power to do this anyway, because other modem functions need it.

B. Performance of the Real-Time Implementation

1) Experimental Results: The main purpose of implementing the system shown in Fig. 22 is to prove that I/Q channel mismatch is no longer a problem in a practical complex single IF receiver even with interference at the image band of the desired signal. Implementing it in real time shows that the computational load is reasonable, driving it for long runs shows that the algorithm is stable, and using real components to generate the bit streams shows that it is robust under the presence of the wide variety of distortions, offsets, drifts, mismatches and noise sources encountered in a real system. In this testing prototype, the interference signals are actually introduced just after the mixers and before the modulator because of the limitation of the components and equipments.

The desired signal used in this example is a GMSK signal with 100-kb/s data rate. The interference signal is an FM signal at 1.912 GHz, and its bandwidth is 100 kHz. After decimation, the image interference will alias into the baseband 0–100 kHz when there is a mismatch in the receiver. Fig. 23 shows the magnitude responses of Y_1 and U_1 (defined in Fig. 22). It can be seen that the image aliasing between 0–100 kHz has been attenuated in Fig. 23(b).

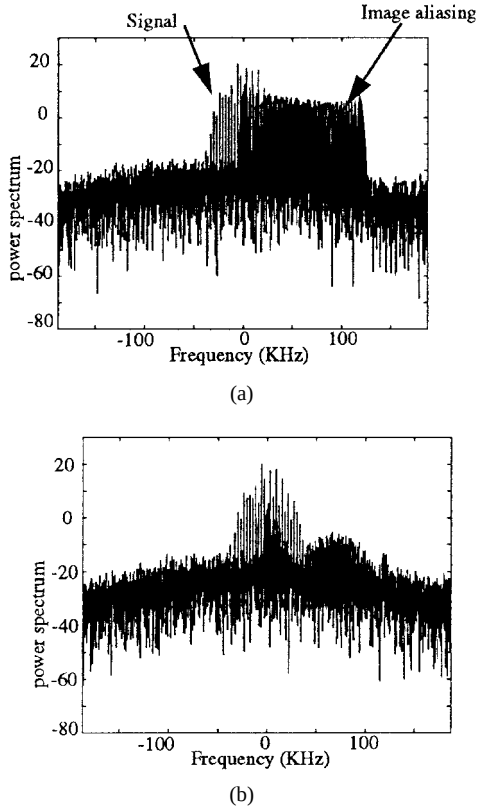

Fig. 23. Magnitude responses of the receiver output—before and after mismatch cancellation (experimental). (a) Magnitude response of Y_1. (b) Magnitude response of U_1.

The comparison has also been done with eye diagrams, as shown in Fig. 24. The eyes are completely closed before applying the mismatch cancellation system. After the mismatch cancellation, we can see the eyes are open which means the

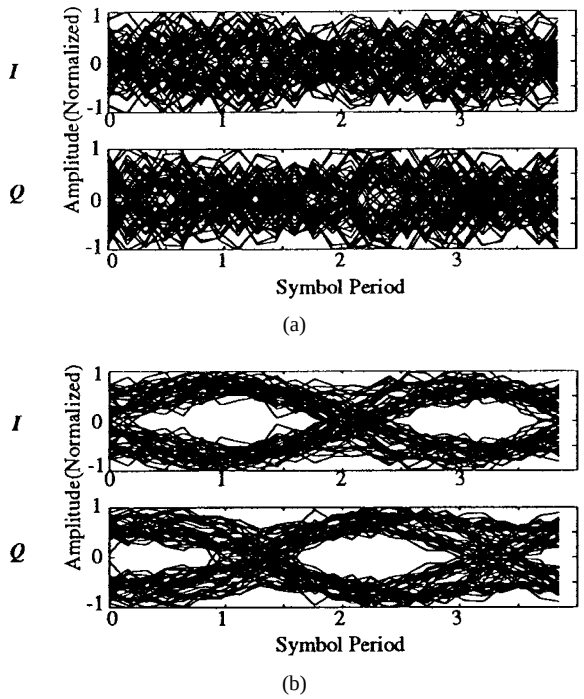

Fig. 24. Eye diagrams for I and Q channels—before and after mismatch cancellation (experimental).

receiver has a reasonable SNR, which in turn allows us to extract the desired information.

We can see from the eye diagrams that there is still some residual noise which makes the eyes unclear. The residual noise comes from two sources: signal leakage and circuit noise. Even though we use the modified version of the adaptive mismatch system, the signal component can not be completely eliminated in the *reference input*. This leakage can impair the performance of the adaptive system. Circuit noise is inherent in the circuits. This kind of noise is uncorrelated with the mismatch effect, thus, we can not use the mismatch cancellation strategy to attenuate it. So signal leakage in the *reference input* and the circuit noise both contribute to the residual noise.

V. Conclusion

This paper addresses I/Q channel mismatch problems in digital receivers and proposes a novel and feasible DSP solution for them without modifying the analog design or using tedious correction procedures.

Image aliasing due to I/Q channel mismatch is always a big concern in realizing quadrature IF receivers. The imbalance between I and Q channels exists along signal paths in subsystems such as the mixer and the modulator. In this paper, quadrature systems were represented as complex systems, therefore, the theories of complex filters and transfer functions have been introduced.

The new DSP system proposed in this paper uses a simple but powerful complex adaptive algorithm to correct the degradation due to the mismatch. A real-time implementation of the new adaptive mismatch cancellation system and a whole complex single IF receiver were presented. The proposed system was implemented in a commercial DSP chip with an interface implemented on the Xilinx FPGA to the receiver front end.

Results from simulations and real-time tests proved the new DSP system is feasible and stable. With the system, the SNR can reach 50 dB, as compared to about 30 dB without it. The dramatic improvement is visible in the magnitude responses and eye diagrams of the I/Q signals. Adaptation characteristics of the new algorithm were also shown in the results.

References

[1] S. Abdennadher *et al.*, "Adaptive self-calibrating delta-sigma modulators," *Electron. Lett.*, vol. 28, pp. 1288–1289, July 1992.
[2] *ADSP 21020 Evaluation Board Manual*, Analog Device Inc., Norwood, MA, 1992.
[3] R. H. Allen, "Complex analog filter obtained from shifted lowpass prototypes," MA.Sc. thesis, Univ. Toronto, ON, Canada, 1985.
[4] P. M. Aziz *et al.*, "Performance of complex noise transfer functions in bandpass and multi band $\Sigma\Delta$ systems" in *Proc. 1995 IEEE ISCAS*, vol. 1, p. 641, May 1995.
[5] S. Bazarjani. (1996). "Mixed analog-digital design considerations in deep submicron CMOS technologies," Ph.D dissertation, Carleton Univ., Ottawa, ON, Canada. [Online]. Available HTTP: http://www.doe.carleton.ca:80/~snelgar/archive/phd/seyfithesis.pdf).
[6] U. Bollinger and W. Vollenweider, "Some experiments on direct-conversion receivers," in *Proc. IEE 5th Int. Conf. Radio Receivers and Associated Systems*, July 1990, pp. 40–44.
[7] J. C. Candy and G. C. Temes, "Oversampling methods for A/D and D/A conversion." New York: IEEE Press, 1992.
[8] A. B. Carlson, *Communication Systems*, 3rd ed. New York: McGraw-Hill, 1986.
[9] G. Cauwenberghs and G. C. Temes, "Adaptive calibration of multiple quantization oversampled A/D converters," in *Proc. IEEE ISCAS'96*, Atlanta, pp. 512–516.
[10] F. E. Churchill, G. W. Ogar, and B. J. Thompson, "The correction of I and Q errors in a coherent processor," *IEEE Trans. Aerosp. Electron. Syst.*, vol. AES-17, pp. 131–137, Jan. 1981.
[11] D. Van Compernolle and S. Van Gerven, "Signal separation in a symmetric adaptive noise canceler by output decorrelation," *IEEE Trans. Signal Processing*, vol. 43, p. 1602, July 1995.
[12] E. B. Hogenauer, "An economical class of digital filters for decimation and interpolation," *IEEE Trans. Acoust., Speech, Signal Processing*, vol. ASSP-29, pp. 155–162, Apr. 1981.
[13] S. Jantzi *et al.*, "Complex bandpass $\Sigma\Delta$ converter for digital radio," in *Proc. 1994 IEEE ISCAS*, London, U.K., May–June 1994, vol. 5, p. 453.
[14] S. A. Jantzi *et al.*, "The effects of mismatch in complex bandpass $\Sigma\Delta$ modulators," in *Proc. ISCAS 1996*, Atlanta, GA, May 1996, p. 227.
[15] E. A. Lee and D. G. Messerschmitt, *Digital Communication*, 2nd ed. Norwell, MA: Kluwer, 1994.
[16] J. R. Long *et al.*, "A low-voltage silicon bipolar RF front-end for PCN receiver applications," *Proc. 1995 ISSCC*, San Francisco, CA, p. 140.
[17] J. Macedo, M. Copeland, and P. Schvan, "A 2.5 GHz monolithic silicon image reject filter," in *Proc. IEEE CICC*, San Diego, CA, 1996.
[18] A. V. Oppenheim and A. S. Willsky, *Signals and Systems*. Englewood Cliffs, NJ: Prentice-Hall, 1983.
[19] A. V. Oppenheim and R. W. Schafer, *Discrete-Time Signal Processing*. Englewood Cliffs, NJ: Prentice-Hall, 1989.
[20] J. G. Proakis, *Digital Communications*, 2nd ed. New York: McGraw-Hill, 1989.
[21] T. S. Rappaport, *Wireless Communications, Principles and Practice*. Englewood Cliffs, NJ: Prentice-Hall, 1996.
[22] W. E. Sabin and E. O. Schoenike, *Single Sideband Systems and Circuits*. New York: McGraw-Hill, 1995.
[23] G. J. Saulnier *et al.*, "A VLSI demodulator for digital RF network applications: Theory and results," *IEEE Trans. Select. Areas Commun.*, vol. 8, p. 1500, Oct. 1990.
[24] R. Schreier and M. Snelgrove, "Decimation for bandpass $\Sigma\Delta$ analog to digital conversion," in *Proc. 1990 ISCAS*, New Orleans, LA, p. 1801.
[25] G. Schultes *et al.*, "Basic performance of a direct-conversion DECT receiver," *Electron. Lett.*, vol. 26, no. 21, pp. 1746–1748, Oct. 1990.
[26] M. Schwartz, *Information Transmission, Modulation and Noise*, 4th ed. New York: McGraw-Hill, 1990.

[27] K. Shenoi, *Digital Signal Processing in Telecommunications*. Englewood Cliffs, NJ: Prentice Hall, 1995.
[28] W. M. Snelgrove, "Intermediate function synthesis," Ph.D. dissertation, Univ. Toronto, ON, Canada, 1982. [Online]. Available HTTP: http://www.doe.carleton.ca:80/˜snelgar/archive/phd/Martinthesis.pdf.
[29] W. M. Snelgrove and L. Yu, preliminary patent disclosure, Aug. 1997.
[30] T. Stetzler *et al.*, "A 2.7 V to 4.5 V single-chip GSM transceiver RF integrated circuit," in *Proc. ISSCC*, 1995, pp. 114–115, 150–151, 354.
[31] A. Swaminathan. (1997). "A single-IF receiver architecture using a complex $\Sigma\Delta$ modulator," M.Eng. thesis, Carleton Univ., Ottawa, ON, Canada. [Online]. Avalable HTTP: http://www.doe.carleton.ca:80/˜snelgar/archive/masters/ASHthesis.pdf
[32] A. Swaminathan and M. Snelgrove *et al.*, "A monolithic complex $\Sigma\Delta$ modulator for digital radio," in *Proc. 1996 IEEE-CAS Region 8 Workshop on Analog and Mixed IC Design*, Pavia, Italy, Sept. 1996, p. 83.
[33] A. Swaminathan and M. Snelgrove, "A single-IF IR radio for PCS," in *Proc. Biennial Symp. Communications*, Kingston, ON, 1996.
[34] H. L. Van Trees, *Detection, Estimation, and Modulation Theory, Part I*. New York: Wiley, 1968.
[35] J. Tsui, *Digital Techniques for Wideband Receivers*. Norwood, MA: Artech House, 1995.
[36] S. A. Vieria-Ribeiro, "Single-IF DECT receiver architecture using a quadrature sub-sampling band-pass $\Sigma\Delta$ modulator," M.Eng. thesis, Carleton Univ., Ottawa, ON, Canada, 1995.
[37] B. Widrow *et al.*, *Adaptive Signal Processing*. Englewood Cliffs, NJ: Prentice-Hall, 1985.
[38] ———, "The complex LMS algorithm," *Proc. IEEE*, vol. 59, p. 719, Apr. 1971.
[39] A. Wiesbauer and G. C. Temes, "On-line digital compensation of analog circuit imperfections for cascaded $\Sigma\Delta$ modulators," in *Proc. 1996 IEEE-CAS Region 8 Workshop on Analog and Mixed IC Design*, Pavia, Italy, p. 92.
[40] H. K. Yang and E. I. El-Masry, "A novel double sampling technique for delta sigma modulators," in *Proc. 37th Midwest Symp. Circuits and Systems*, Lafeyette, LA, Aug. 1994.
[41] L. Yu and M. Snelgrove, "Mismatch cancellation for complex bandpass $\Sigma\Delta$ modulators," in *Proc. 40th Midwest Symp. Circuits and Systems*, Sacramento, CA, Aug. 1997, pp. 814–818.
[42] L. Yu, "A novel adaptive mismatch cancellation system for quadrature IF radio receivers," M.Eng. thesis, Oct. 1997. [Online]. Available HTTP: http://www.doe.carleton.ca:80/˜snelgar/archive/CV/CV2.pdf

Li Yu (M'98) received the B.Eng. degree in electronic engineering from Tsinghua University, Beijing, China., in 1993, and the M.Eng. degree in electronic engineering in 1997 from Carleton University, Ottawa, ON, Canada.

She currently works as an ASIC designer at Nortel Networks Corporation, Ottawa, ON, Canada, where she is involved in developing and implementing architectures and circuits for telecommunications and data communications. Her research interests include adaptive analog and digital signal processing, highly parallel architectures for signal processing, and radio receiver architectures and circuits.

W. Martin Snelgrove (S'75–M'78) , for a photograph and biography, see p. 389 of the April 1999 issue of this TRANSACTIONS.